



ELSEVIER

Contents lists available at ScienceDirect

Advances in Mathematics

www.elsevier.com/locate/aim



Smooth polyhedral surfaces

Felix Günther^{a,b,c,*}, Caigui Jiang^{d,e}, Helmut Pottmann^{e,f}



^a Erwin Schrödinger International Institute for Mathematical Physics,
Boltzmannngasse 9, 1090 Vienna, Austria

^b Max Planck Institute for Mathematics, Vivatsgasse 7, 53111 Bonn, Germany

^c Institut für Mathematik, MA 8-3, Technische Universität Berlin, Straße des 17.
Juni 136, 10623 Berlin, Germany

^d Max Planck Institute for Informatics, Campus E1 4, 66123 Saarbrücken,
Germany

^e Visual Computing Center, Building 1, 4700 King Abdullah University of Science
and Technology, Thuwal 23955-6900, Saudi Arabia

^f Center for Geometry and Computational Design, Technische Universität Wien,
Wiedner Hauptstraße 8/104, 1040 Vienna, Austria

ARTICLE INFO

Article history:

Received 20 March 2017

Received in revised form 4 November
2019

Accepted 6 January 2020

Available online xxxx

Communicated by Ezra Miller

MSC:

52B70

53A05

Keywords:

Discrete differential geometry

Polyhedral surface

Smoothness

Discrete Gaussian curvature

Asymptotic direction

Projective transformation

ABSTRACT

Polyhedral surfaces are fundamental objects in architectural geometry and industrial design. Whereas closeness of a given mesh to a smooth reference surface and its suitability for numerical simulations were already studied extensively, the aim of our work is to find and to discuss suitable assessments of smoothness of polyhedral surfaces that only take the geometry of the polyhedral surface itself into account. Motivated by analogies to classical differential geometry, we propose a theory of smoothness of polyhedral surfaces including suitable notions of normal vectors, tangent planes, asymptotic directions, and parabolic curves that are invariant under projective transformations. It is remarkable that seemingly mild conditions significantly limit the shapes of faces of a smooth polyhedral surface. Besides being of theoretical interest, we believe that smoothness of polyhedral

* Corresponding author at: Institut für Mathematik, MA 8-3, Technische Universität Berlin, Straße des 17. Juni 136, 10623 Berlin, Germany.

E-mail addresses: fguenth@math.tu-berlin.de (F. Günther), caigui.jiang@kaust.edu.sa (C. Jiang), helmut.pottmann@kaust.edu.sa (H. Pottmann).

surfaces is of interest in the architectural context, where vertices and edges of polyhedral surfaces are highly visible.

© 2020 Elsevier Inc. All rights reserved.

1. Introduction

In modern architecture, facades and glass roofs often model smooth shapes but are realized as polyhedral surfaces. Bad approximations may be observed as wiggly meshes, even though the polyhedral mesh is close to a smooth reference surface. High demands on the aesthetics of the realized surface necessitate adequate assessments of smoothness. But what does it mean for a polyhedral surface to be smooth?

Reflective surfaces visibly expose the kink angles between adjacent faces. A reflection pattern that does not closely follow the actual shape of the polyhedral surface is not appealing to the human eye and may serve as a subjective assessment of smoothness, see Fig. 1. The reflections of parallel light rays are determined by the face normals of the polyhedral surface. So if we are looking for a reflection pattern that is reasonably aligned with the shape of the surface, the Gauss image should contain as few degeneracies such as overlaps and self-intersections as possible. Indeed, the different reflections of the two meshes depicted in Fig. 1 exactly correspond to the different behavior of their Gauss images. Our first requirement for smoothness of a polyhedral surface will be therefore the absence of self-intersections in its Gauss image.

1.1. Prior work

In [5] the design and optimization of polyhedral patterns, which are patterns of planar polygonal faces on freeform surfaces, were studied. It turned out that some patterns adapt their shape according to the sign of Gaussian curvature and others do not. Polyhedral patterns of the first type look smoother than patterns of the other type and are better suitable to approximate smooth surfaces.

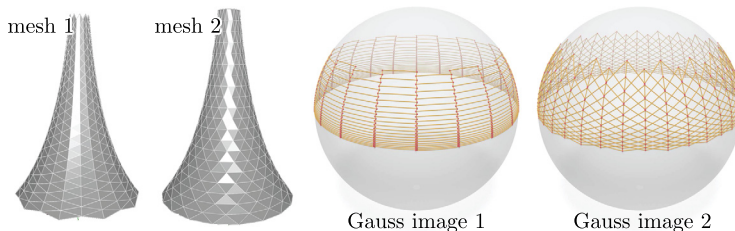


Fig. 1. Evaluation of reflections as a subjective assessment of smoothness: The observation that the reflection pattern of mesh 1 behaves better than the reflections of mesh 2 is encoded in the regularity of its Gauss image.

Orden et al. [7] investigated planar frameworks of forces in static equilibrium. For a planar graph with forces in equilibrium, one can rearrange the forces at each vertex to obtain polygons of forces that themselves can be arranged to form a realization of the dual graph. This realization is called the reciprocal framework. The authors derived conditions on the shapes of polygons and the sign of forces (tension or compression) such that both the original and the reciprocal framework are free of self-intersections. The framework on a planar graph can be viewed as a projection of a (possibly self-intersecting) polyhedron in Euclidean space onto a plane. The dihedral angles correspond to forces, such that inflection faces are encoded by sign changes of the forces. The reciprocal is then the projection of the polar of the original polyhedron, where polarity with respect to the paraboloid $z = x^2 + y^2$ is considered. The result of [7] is that the only planar faces which produce a reciprocal without self-intersections are convex polygons, pseudo-quadrilaterals, and pseudo-triangles, where zero, four, or two or four sign changes appear, respectively.

The first author and Banchoff [2] studied the Gauss image of polyhedral vertex stars. They proved that if the Gauss image has no self-intersections, then its only possible shapes are convex spherical polygons in the case of positive discrete Gaussian curvature and spherical pseudo-digons, -triangles, and -quadrilaterals in the case of negative discrete Gaussian curvature. If one restricts to vertex stars that exhibit a so-called transverse plane onto which they orthogonally project in a one-to-one way, then spherical pseudo-digons do not appear as Gauss images and the result of [7] is recovered.

1.2. Contributions and overview

The aim of our paper is to find suitable assessments of smoothness of polyhedral surfaces without a smooth reference surface. The property we start with in Section 2 is that the Gauss image of the star of a vertex of either positive or negative discrete Gaussian curvature shall have no self-intersections. Whereas the normal of a transverse plane is a suitable normal, we propose a possibly different tangent plane that is motivated by a discretization of the Dupin indicatrix. In the smooth theory, planes parallel and close to the tangent plane at a point of positive or negative curvature intersect the surface in curves that resemble ellipses and hyperbolas, respectively. A similar behavior in the discrete setup is achieved when the Gauss image of a negatively curved vertex star is star-shaped. A normal vector with respect to which the Gauss image is star-shaped then defines a suitable tangent plane. As a result, the asymptotic directions lie within the inflection faces of the vertex star.

Assessing smoothness around a face in Section 3 leads to similar observations. For example, in regions of negative curvature the polyhedral faces have to be pseudo-triangles or -quadrilaterals. The fact that they are dual to the shapes of Gauss images of vertex stars lies in the projective invariance of our notion that is discussed later. This also explains the analogy to [7]. Where we are relating angles of the face to spherical angles, Orden et al. considered the planar angles in the reciprocal vertex star, corresponding to the projective dual described in Theorem 11. They used the fact that the face is an

interior face of the framework, translating to the face being a transverse plane for its neighborhood. In that situation, we can apply the dualization of Theorem 11. In contrast, our arguments are valid even if this theorem cannot be applied.

In addition, we define asymptotic directions in star-shaped faces of negative discrete Gaussian curvature. By demanding that there exists a line segment inside the face that connects the two edges where the discrete Gaussian curvature changes its sign, we limit the shapes of faces with vertices of positive and of negative curvature and define a discrete parabolic curve.

The notion we finally propose for a smooth polyhedral surface can be found in Section 3.4. We demand that the discrete Gaussian curvature is non-zero for all vertices and that its sign changes at either zero or two edges of a face. Furthermore, the Gauss images of all interior vertex stars shall be star-shaped and contained in open hemispheres. For each face, the interior angles of Gauss images of neighboring vertex stars shall add up to 2π or 0 depending on whether the discrete Gaussian curvature has the same sign for all vertices or not. In the first case, we demand in addition that f is star-shaped; in the latter case, we require that the vertices of positive and negative curvature can be separated by a line segment that lies inside the face.

In Section 4, we show that our notion of smooth polyhedral surfaces is projectively invariant. Projective transformations map discrete tangent planes, asymptotic directions, and parabolic curves to the corresponding objects of the image surface. Certain duality properties such as the similar shapes of faces of a negatively curved smooth polyhedral surface and of its Gauss image are reflected by the fact that the projective dual of a negatively curved smooth polyhedral surface is again a negatively curved smooth polyhedral surface.

Finally, we would like to remark that the optimization of a given polyhedral surface approximating a given smooth reference surface toward greater smoothness in the sense of star-shaped Gauss images is the objective of the paper [4] for which the current paper lays the theoretical foundation. A different optimization approach that also bases on Gauss images without self-intersections is presented in the recent paper [8]. Both papers discuss possible applications in the architectural context.

2. Gauss image of vertex stars

In this section, we investigate the Gauss image of a polyhedral vertex star and propose conditions that correspond to smoothness. Our discussion bases on recent results in [2]. The authors proved that the algebraic area enclosed by the Gauss image of a polyhedral vertex star equals the discrete Gaussian curvature of this vertex. Based on this theorem, they derived the possible shapes of Gauss images. We cite their result of the shapes of Gauss images without self-intersections in Theorem 2.

We start with some basic notation in Section 2.1 and continue with a summary of the relevant results of [2] in Section 2.2. The discrete Dupin indicatrices and asymptotic directions are investigated in Section 2.3.

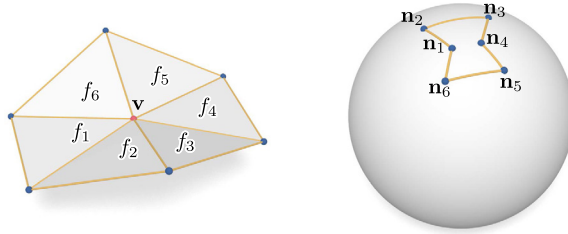


Fig. 2. A vertex star and its Gauss image for negative discrete Gaussian curvature.

2.1. Notation

Let P be an orientable polyhedral surface immersed into three-dimensional Euclidean space. That means, we consider a connected 2-manifold that is a union of polygonal regions such that each vertex of P possesses a neighborhood that is embedded in \mathbb{R}^3 . We do not require any specific condition on the faces f of P besides being simple and planar, but we assume that faces that share an edge are not coplanar and that no interior angle equals π . In particular, faces can be non-convex. Clearly, non-convex faces do not occur in simplicial, i.e., triangulated surfaces, but the faces of the projective dual of a triangular surface have in general more than three vertices and non-convexity usually arises in areas of negative discrete Gaussian curvature.

A vertex of P shall be denoted by \mathbf{v} . In what follows, \mathbf{v} should always be an interior vertex of P , boundary vertices will not be considered. Two vertices \mathbf{v}_1 and \mathbf{v}_2 are adjacent if they are connected by an edge, two faces f_1 and f_2 are adjacent if they share an edge. A face f or an edge e is incident to a vertex \mathbf{v} , if the vertex is a corner of the face or the edge, respectively. For adjacency and incidence we will use the notations $\mathbf{v}_1 \sim \mathbf{v}_2$, $f_1 \sim f_2$ and $f, e \sim \mathbf{v}$, $\mathbf{v} \sim f, e$, respectively. \mathbf{v} is said to be convex, if the star of \mathbf{v} determines the boundary of a convex polyhedral cone.

We fix one orientation of P and denote by $\mathbf{n}_f \in S^2$ the outer unit normal vector of a face f . For an interior vertex \mathbf{v} , we connect the normals of adjacent faces $\mathbf{n}_{s-1}, \mathbf{n}_s \sim \mathbf{v}$ by the shorter of the two great circle arcs connecting \mathbf{n}_{s-1} and \mathbf{n}_s . Since P is immersed, $\mathbf{n}_{s-1} \neq \pm \mathbf{n}_s$, so the shorter arc is non-trivial and well defined. Hence, the normals \mathbf{n}_f for $f \sim \mathbf{v}$ define a spherical polygon $g(\mathbf{v})$ that we call the Gauss image of the vertex star, see Fig. 2.

Definition. For a fixed vertex \mathbf{v} , let α_f denote the interior angle of an incident face f at \mathbf{v} . The discrete Gaussian curvature at \mathbf{v} is defined as the angle deficit

$$K(\mathbf{v}) := 2\pi - \sum_{f \sim \mathbf{v}} \alpha_f.$$

Definition. Let f be a face of the star of the vertex \mathbf{v} . If the two other faces of the vertex star that are adjacent to f lie in different half-spaces that the plane through f determines, then f is said to be an inflection face.

2.2. Gauss images without self-intersection

In order to derive the shape of a Gauss image from the equality of its area and the discrete Gaussian curvature of the underlying vertex star, the following lemma was important in the paper [2] and is also useful in our investigation.

Lemma 1. *Let $f_1, f_2, f_3 \sim \mathbf{v}$ be three consecutive faces that are ordered in counterclockwise direction around \mathbf{v} with respect to the given orientation of P . Let $\alpha = \alpha_2$ be the angle of f_2 at \mathbf{v} and α' the spherical angle $\angle \mathbf{n}_3 \mathbf{n}_2 \mathbf{n}_1$.*

- (i) *If $\alpha < \pi$ and f_2 is not an inflection face, then $\alpha' = \pi - \alpha$.*
- (ii) *If $\alpha < \pi$ and f_2 is an inflection face, then $\alpha' = 2\pi - \alpha$.*
- (iii) *If $\alpha > \pi$ and f_2 is not an inflection face, then $\alpha' = 3\pi - \alpha$.*
- (iv) *If $\alpha > \pi$ and f_2 is an inflection face, then $\alpha' = 2\pi - \alpha$.*

In the smooth theory, the Gauss map is locally injective in areas of non-zero curvature. In the case of positive Gaussian curvature, the Gauss map is orientation-preserving; in the case of negative curvature it is orientation-reversing. So a natural requirement for *smoothness* of a polyhedral surface is that if $K(\mathbf{v})$ is non-zero, then $g(\mathbf{v})$ shall have no self-intersections as in Fig. 2.

The shape of Gauss images without self-intersection was considered in [2]. The authors showed that in the case of positive discrete Gaussian curvature, the Gauss image can only be a convex spherical polygon, and in the case of negative curvature, only spherical pseudo- n -gons with $n = 2, 3, 4$ occur.

Definition. A spherical polygon without self-intersections is called a *pseudo- n -gon*, if exactly n of its interior angles are less than π . The corresponding n vertices are called *corners*.

Theorem 2. *Assume that the Gauss image $g(\mathbf{v})$ has no self-intersections.*

- (i) *If the discrete Gaussian curvature $K(\mathbf{v})$ is positive, then the star of \mathbf{v} is convex and the Gauss image $g(\mathbf{v})$ is a convex spherical polygon, see Fig. 3.*
- (ii) *If $K(\mathbf{v}) < 0$ and the angle α_f of any face $f \sim \mathbf{v}$ at \mathbf{v} is less than π , then $g(\mathbf{v})$ is a spherical pseudo-quadrilateral, see Fig. 4. Its four corners are the normals of the exactly four inflection faces in the star of \mathbf{v} .*
- (iii) *If $K(\mathbf{v}) < 0$ and $\alpha_f > \pi$ for exactly one $f \sim \mathbf{v}$, then $g(\mathbf{v})$ is a spherical pseudo-triangle. If this face f is an inflection face, then the three corners of $g(\mathbf{v})$ are the normals of the other three inflection faces, see Fig. 5. If f is not an inflection face, then \mathbf{n}_f and the normals of the only two inflection faces in the star of \mathbf{v} are the three corners of $g(\mathbf{v})$, see Fig. 6.*

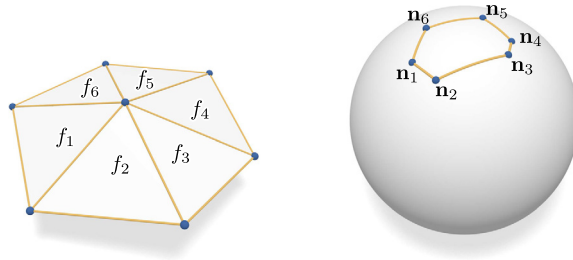


Fig. 3. $g(\mathbf{v})$ is a convex spherical polygon.

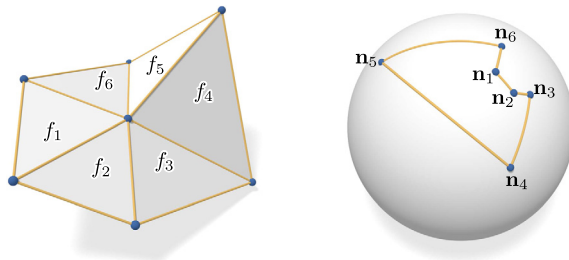


Fig. 4. $g(\mathbf{v})$ is a spherical pseudo-quadrilateral, f_3, f_4, f_5, f_6 are inflection faces.

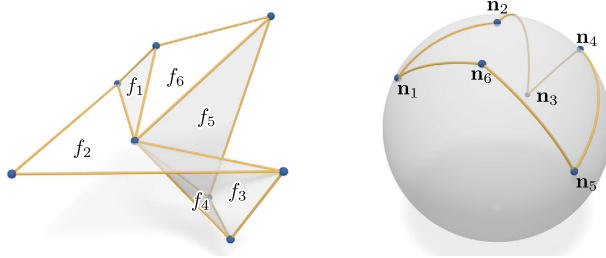


Fig. 5. $g(\mathbf{v})$ is a spherical pseudo-triangle, f_1, f_2, f_3, f_5 are inflection faces.

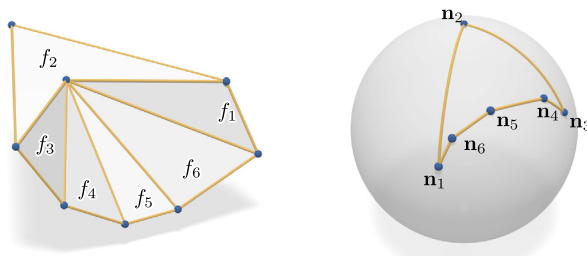


Fig. 6. $g(\mathbf{v})$ is a spherical pseudo-triangle, f_1, f_4 are inflection faces.

(iv) If $K(\mathbf{v}) < 0$ and $\alpha_f > \pi$ for more than one $f \sim \mathbf{v}$, then $g(\mathbf{v})$ is a spherical pseudo-digon, see Fig. 7. There are exactly two faces f such that $\alpha_f > \pi$ and these two

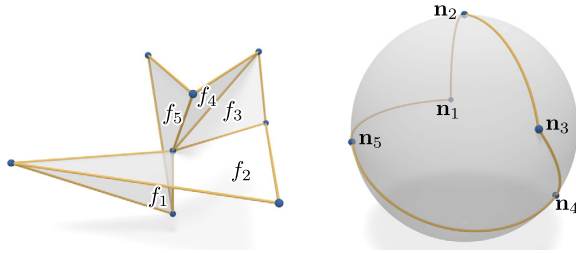


Fig. 7. $g(\mathbf{v})$ is a spherical pseudo-digon, f_1, f_2, f_4, f_5 are inflection faces.

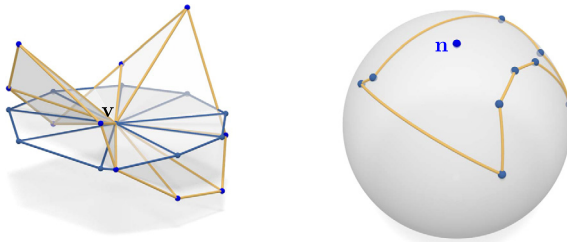


Fig. 8. Relation between the existence of a transverse plane and the Gauss image.

faces are inflection faces. The two corners of $g(\mathbf{v})$ are the normals of the other two inflection faces in the vertex star.

A smooth surface locally projects to the tangent plane at a point in a bijective way. Theorem 2 (iv) describes an example where the discrete analogue is actually not true. The corresponding discrete concept of a transverse plane goes back to Banchoff. The following characterization of the existence of a transverse plane in terms of the Gauss image was proved in [2], see Fig. 8.

Definition. A plane E passing through a vertex \mathbf{v} of the polyhedral surface P is said to be a *transverse plane* if a disk neighborhood of the star of \mathbf{v} projects orthogonally to E in a one-to-one way.

Proposition 3. *There exists a transverse plane through a vertex \mathbf{v} of P if and only if the Gauss image $g(\mathbf{v})$ is contained in an open hemisphere.*

Note that it easily follows from Theorem 2 (i) that $g(\mathbf{v})$ is contained in an open hemisphere if it has no self-intersections and $K(\mathbf{v}) > 0$. So this assumption is only a restriction in the case of negative discrete Gaussian curvature.

Corollary 4. *Let \mathbf{v} be a vertex of P such that $K(\mathbf{v}) < 0$ and $g(\mathbf{v})$ is contained in an open hemisphere. Then, $g(\mathbf{v})$ is not a spherical pseudo-digon.*

Proof. By Proposition 3, there is a plane E such that a disk neighborhood of the star of \mathbf{v} projects orthogonally to E in a one-to-one way. Under orthogonal projection, any

reflex angle will be mapped to a reflex angle (or a straight angle in the degenerate case). It follows that the star of \mathbf{v} contains at most one face f with $\alpha_f > \pi$. In particular, $g(\mathbf{v})$ cannot be a spherical pseudo-digon due to the classification result in Theorem 2. \square

So a good assertion for smoothness of a polyhedral vertex star to start with is that the Gauss image has no self-intersections and is contained in an open hemisphere. The pole of such a hemisphere then serves as a discrete normal.

Definition. Let \mathbf{v} be a vertex of P and assume that $g(\mathbf{v})$ is contained in an open hemisphere with pole \mathbf{n} inside $g(\mathbf{v})$. Then, \mathbf{n} is said to be a *discrete normal*.

2.3. Discrete Dupin indicatrices and asymptotic directions

In the smooth theory, the Dupin indicatrix indicates how the intersection of the surface with a plane parallel and close to the tangent plane through a point looks like. The Dupin indicatrix is the limit of the intersections when the planes are approaching the tangent plane. It is an ellipse if the Gaussian curvature is positive and a hyperbola if the Gaussian curvature is negative. In the latter case, the asymptotic directions at a point are the asymptotes of the Dupin indicatrix.

In the following, we discuss a discrete analog of the Dupin indicatrix for polyhedral surfaces. In the case of positive discrete Gaussian curvature, the best discrete Dupin indicatrix that we can hope for is a convex polygon. This is indeed the case and an immediate consequence of Theorem 2 (i):

Proposition 5. *Assume that $K(\mathbf{v}) > 0$ and that $g(\mathbf{v})$ has no self-intersections. Then, $g(\mathbf{v})$ is star-shaped with respect to any point $\mathbf{n} \in S^2$ in its interior. If a plane E orthogonal to \mathbf{n} and close to (but not passing through) \mathbf{v} has a non-trivial intersection with the star of \mathbf{v} , then the intersection is a convex polygon.*

In the case of negative discrete Gaussian curvature, we derive exactly the condition of $g(\mathbf{v})$ being star-shaped with respect to $\mathbf{n} \in S^2$ that guarantees that the intersections orthogonal to \mathbf{n} and close to \mathbf{v} discretize hyperbolas.

Definition. A *discrete hyperbola* is the union of two (possibly infinite) simple polylines, none of which contains an inflection edge, such that the convex hulls of the polylines are disjoint as in Fig. 10.

Remark. Note that the discrete hyperbolas that we defined only have the shape of a hyperbola, but do not share their properties. For example, a line may intersect a discrete hyperbola in three points.

For simplicity, we assume for the following theorem that the faces of the star V of a vertex \mathbf{v} are (infinite) cones. A reflex angle is decomposed into two convex cones.

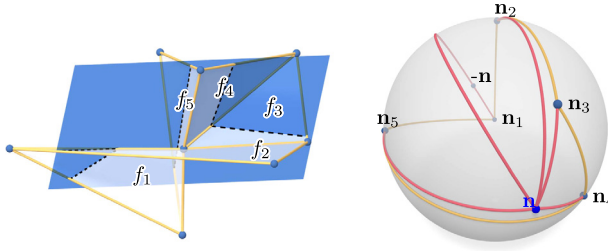


Fig. 9. The intersection consists of three components when $-\mathbf{n}$ is contained in $g(\mathbf{v})$.

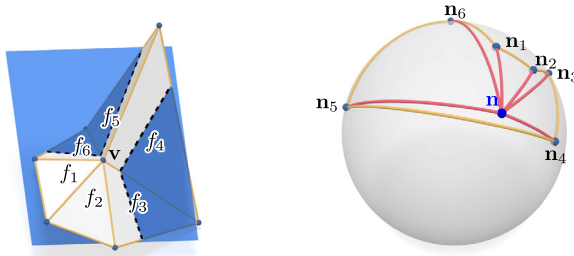


Fig. 10. Discrete Dupin indicatrix is a discrete hyperbola if the Gauss image is star-shaped.

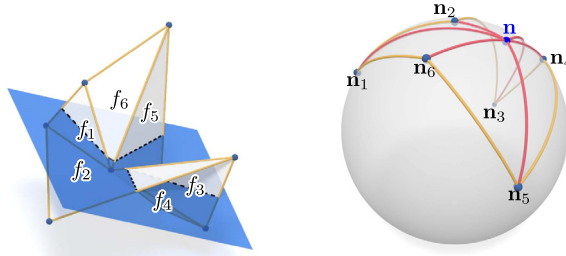


Fig. 11. Discrete Dupin indicatrix is a discrete hyperbola if the Gauss image is star-shaped (case of a spherical pseudo-triangle).

Theorem 6. Assume that $K(\mathbf{v}) < 0$ and that $g(\mathbf{v})$ has no self-intersections. Let $\mathbf{n} \in S^2$ be a point in its interior and E be a plane orthogonal to \mathbf{n} and not passing through \mathbf{v} .

- (i) If $-\mathbf{n}$ is contained in $g(\mathbf{v})$, then the intersection of E with V has three connected components as in Fig. 9.
- (ii) If $-\mathbf{n}$ is not contained in $g(\mathbf{v})$, then the intersection of E with V consists of two distinct polylines. If and only if $g(\mathbf{v})$ is star-shaped with respect to \mathbf{n} , then this intersection is a discrete hyperbola as in Figs. 10 and 11. There exist planes E such that one of the polylines is a single straight line segment if and only if the vertex star contains a face f with $\alpha_f > \pi$ that is not an inflection face, see Fig. 12.

Proof. For $\mathbf{n} \in S^2$ inside $g(\mathbf{v})$, let E_0 be the plane that is orthogonal to \mathbf{n} and passing through \mathbf{v} . Let $i(\mathbf{v}, \mathbf{n}) := 1 - F/2$, where F is the number of cones in the vertex star

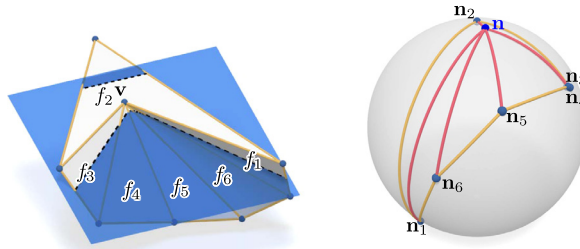


Fig. 12. The intersection is a discrete hyperbola, one polyline is a straight line segment.

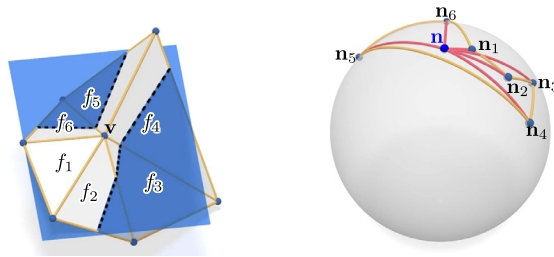


Fig. 13. An inflection edge appears in the intersection if the Gauss image is not star-shaped with respect to \mathbf{n} .

that E_0 intersects non-trivially. $i(\mathbf{v}, \mathbf{n})$ coincides with the critical point index that was introduced by Banchoff in [1]. In [2], it is shown that $i(\mathbf{v}, \mathbf{n})$ equals the sum of winding numbers of $\pm \mathbf{n}$ with respect to $g(\mathbf{v})$.

If \mathbf{n} and $-\mathbf{n}$ are both contained in $g(\mathbf{v})$, then their winding numbers are -1 . Thus, $i(\mathbf{v}, \mathbf{n}) = -2$, so E_0 intersects six cones of V . This leads to three connected components in the intersection of the plane E with V .

If $-\mathbf{n}$ is not contained in $g(\mathbf{v})$, its winding number is 0 and $i(\mathbf{v}, \mathbf{n}) = -1$. In particular, E_0 intersects exactly four cones of V and the intersection of E with V consists of two polylines. These two polylines each bound a convex set if and only if no polyline contains an inflection edge. An inflection edge can only occur if E intersects an inflection face of V and both its neighboring faces as in Fig. 13. Equivalently, E_0 intersects this inflection face in \mathbf{v} only. We deduce that the intersection of E with V consists of two convex polylines if and only if E_0 intersects all inflection faces non-trivially.

It is not hard to see that a face f with interior angle $\alpha_f < \pi$ at \mathbf{v} is intersected non-trivially by E_0 if and only if \mathbf{n} is contained in the double lune with vertices $\pm \mathbf{n}_f$ and opening angle α_f that is bounded by the great circles passing through the arcs of $g(\mathbf{v})$ incident to \mathbf{n}_f , see for example [1].

By Theorem 2, $g(\mathbf{v})$ is a spherical pseudo- n -gon and its corners are the normals of the inflection faces f with interior angle $\alpha_f < \pi$ or the normal of a non-inflection face f with interior angle $\alpha_f > \pi$.

Let us first consider the case that any face f with angle $\alpha_f > \pi$ is an inflection face as in Fig. 10. Equivalently, this is the case with exactly four inflection faces. $g(\mathbf{v})$ is star-shaped with respect to \mathbf{n} if and only if its corners can be seen from \mathbf{n} . This is exactly

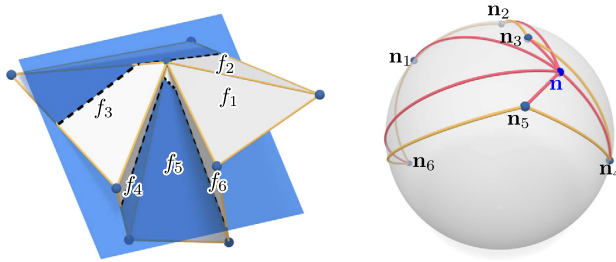


Fig. 14. Polyline bound convex sets such that one is containing the other.

the case when all inflection faces are non-trivially intersected by E_0 , observing that a face f with angle $\alpha_f > \pi$ is intersected by E_0 in any case. It is also easy to see that the intersection of E_0 with such a face cannot be a line segment containing \mathbf{v} . Thus, the intersection of E with V consists of two convex polylines of at least two edges.

It remains to show that the two polylines bound disjoint convex sets. Equivalently, the angle between any two consecutive line segments in the intersection of E_0 with V is less than π . Let E_0 intersect f and f' in consecutive order. The angle between the line segments equals $\pi - \angle \mathbf{n}_{f'} \mathbf{n}_f$. This angle is contained in $(0, \pi)$ because $g(\mathbf{v})$ is star-shaped with respect to \mathbf{n} .

We now come to the case that the vertex star contains only two inflection faces or, equivalently, that there is a face f with a reflex angle that is not an inflection face. Then, $g(\mathbf{v})$ is a spherical pseudo-triangle, two of its corners correspond to inflection faces and the other corner is \mathbf{n}_f . By our observations above, the two polylines in the intersection of E with V bound convex sets if and only if the two corners different from \mathbf{n}_f can be seen from \mathbf{n} .

Assume first that \mathbf{n}_f can be seen from \mathbf{n} . Then, E_0 intersects f in a line segment with \mathbf{v} in its interior. It follows that the convex sets which the two polylines in the intersection of E with V bound are disjoint and that one of the polylines is a straight line segment if \mathbf{v} is on the appropriate side of E .

Now, assume that \mathbf{n}_f cannot be seen from \mathbf{n} , see Fig. 12. Then, E_0 intersects f in a line segment starting in \mathbf{n} . Since E_0 intersects four cones of V non-trivially, it follows that it intersects also a non-inflection face f' . Hence, \mathbf{n} lies in the corresponding double lune with vertices $\pm \mathbf{n}_{f'}$ and opening angle $\alpha_{f'}$. In particular, if we compare the orientation of the faces around the vertex star with the reversed orientation of its normals as seen from \mathbf{n} , then the order of \mathbf{n}_f and $\mathbf{n}_{f'}$ is interchanged.

Clearly, the line segments corresponding to f and f' that appear in the intersection of E_0 with V are consecutive if one goes along the vertex star, say f' comes after f in counterclockwise direction. The angle α between them is given by $\pi - \angle \mathbf{n}_{f'} \mathbf{n}_f$. But now, $0 > \angle \mathbf{n}_{f'} \mathbf{n}_f$, so $\alpha > \pi$. Thus, for suitable E the two polylines bound convex sets containing each other, see Fig. 14. \square

Note that if the Gauss image is contained in an open hemisphere, case (i) of Theorem 6 is excluded by Corollary 4. Motivated by the existence of a transverse plane in

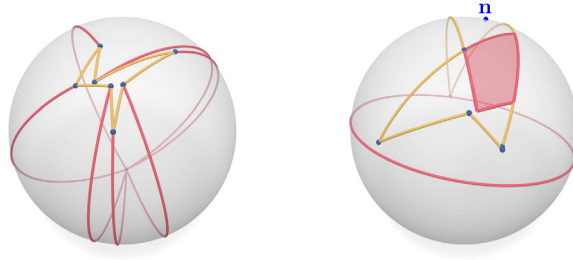


Fig. 15. Gauss images that are star-shaped only with respect to the exterior (left) or where no pole of an open hemisphere containing it is in the kernel (right).

Proposition 3 and by the discrete Dupin indicatrix in Theorem 6, we propose the following notion of a smooth polyhedral vertex star and of discrete asymptotic directions:

Definition. The star of an interior point \mathbf{v} of P is said to be *smooth*, if there exist $\mathbf{n}, \mathbf{n}' \in S^2$ inside the Gauss image $g(\mathbf{v})$ such that it is star-shaped with respect to \mathbf{n} and contained in the open hemisphere with pole \mathbf{n}' . A plane orthogonal to \mathbf{n} and passing through \mathbf{v} defines a *discrete tangent plane*. If $K(\mathbf{v}) < 0$, the directions defined by the four line segments in the intersection of the discrete tangent plane with a disk neighborhood of \mathbf{v} are said to be *discrete asymptotic directions*.

In particular, asymptotic directions lie in the planar cone spanned by the edges incident to \mathbf{v} of an inflection face $f \sim \mathbf{v}$ with angle $\alpha_f < \pi$, in the opposite of this cone if f is an inflection face with angle $\alpha_f > \pi$, and in the double cone spanned by one edge and the inverse of the other if f is a non-inflection face with angle $\alpha_f > \pi$.

Remark. Note that algorithmically, star-shapedness can be checked more easily than freeness of self-intersections [4]. We also remark that star-shapedness with respect to some point on S^2 does not imply star-shapedness with respect to an interior point, see Fig. 15. The figure also shows that it may happen that the normal of a discrete tangent plane may never be a discrete normal. However, this will not happen if the Gauss image is small enough. Still, these concepts should be treated differently since projective transformations map lines to lines and planes to planes, but do not preserve angles.

3. Gauss images around faces and shapes of faces

After having identified smoothness of vertex stars by the star-shapedness of their Gauss images, we now assess smoothness of the neighborhood of an interior face f of a polyhedral surface P . Our basic idea is that the Gauss images of stars of vertices $\mathbf{v} \sim f$ shall arrange at \mathbf{n}_f with as few overlaps as possible. The case of positive discrete Gaussian curvature in Section 3.1 then leads to convex polyhedra; in the negative curvature case, we deduce in Section 3.2 that smoothness demands the faces to be pseudo-triangles

or -quadrilaterals. Star-shapedness of the face allows us to define discrete asymptotic directions within the face. Faces with vertices of both positive and negative discrete Gaussian curvature and discrete parabolic curves separating them are discussed in Section 3.3. We conclude with our definition of a smooth polyhedral surface in Section 3.4 and compare our notions of discrete asymptotic directions and discrete parabolic curves with their smooth counterparts on a Dupin cyclide in Section 3.5.

A smooth surface of vanishing Gaussian curvature is developable. The study of discrete developable surfaces is not the aim of our exposition and for the modeling of discrete developable surfaces using polyhedral surfaces with quadrilateral faces we refer for example to [6]. For this reason, we assume that $K(\mathbf{v}) \neq 0$ for all \mathbf{v} . Since the faces of P are flat, it is also quite natural to locate the *parabolic* points (points of zero Gaussian curvature) on the faces and not on the vertices.

Our main interest lies in generic parabolic points. Isolated parabolic points, which occur for example on a monkey saddle, are not generic since a small perturbation deforms the isolated parabolic point into a closed parabolic curve. Even though we can model polyhedral monkey saddles around faces in Section 3.2, we do not include such saddles in our notion of smoothness.

3.1. Region of positive discrete Gaussian curvature

Proposition 7. *Assume that $K(\mathbf{v}) > 0$ and that the Gauss image $g(\mathbf{v})$ has no self-intersections for any vertex \mathbf{v} of the interior face f . Then, f is a convex polygon and the Gauss images $g(\mathbf{v})$ do not intersect each other.*

Proof. By Theorem 2, the star of any vertex \mathbf{v} of f is convex. It follows that f is a convex polygon and that the neighborhood of f forms a part of a convex polyhedron. From Lemma 1 we deduce that the angle of $g(\mathbf{v})$ at \mathbf{n}_f equals $\pi - \alpha_{\mathbf{v}}$, where $\alpha_{\mathbf{v}}$ denotes the interior angle of f at \mathbf{v} . Then, the angles of the Gauss images of the n vertex stars at \mathbf{n}_f add up to

$$\sum_{\mathbf{v} \sim f} (\pi - \alpha_{\mathbf{v}}) = n\pi - \sum_{\mathbf{v} \sim f} \alpha_{\mathbf{v}} = n\pi - (n - 2)\pi = 2\pi.$$

It follows that the Gauss images of the vertex stars, which are convex spherical polygons, arrange at \mathbf{n}_f without any overlaps. \square

Whereas we have a choice of the tangent plane through a vertex of the polyhedral surface that serves as the unique point of contact, the plane through a face is a unique tangent plane, but there is a choice of the point of contact.

Definition. Let f be a convex face of the polyhedral surface P . Then, any interior point of f can serve as the *point of contact* of the *discrete tangent plane* given by the plane through f .

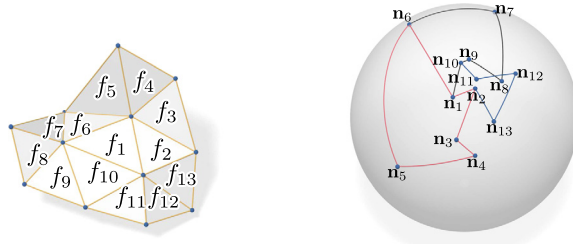


Fig. 16. Gauss images of the stars of the vertices of $f = f_1$ do not overlap around \mathbf{n}_1 : f_9 and f_{10} are not inflection faces in the left vertex star, f_2 and f_{11} are not inflection faces in the lower vertex star, and f_1 and f_3 are not inflection faces in the upper vertex star.

3.2. Region of negative discrete Gaussian curvature

Let us now assume that $K(\mathbf{v}) < 0$ and that the Gauss image $g(\mathbf{v})$ has no self-intersections for any vertex $\mathbf{v} \sim f$. If we go around the vertices of f in counterclockwise order, the corresponding Gauss images are attached at \mathbf{n}_f in clockwise order. Our condition for smoothness is that the Gauss images shall not overlap near \mathbf{n}_f , meaning that their interior angles sum up to 2π . Note that in contrast to Proposition 7, the Gauss images may now intersect away from \mathbf{n}_f as in Fig. 16. However, only transversal intersections are possible. This requires the two intersecting Gauss images to enclose a region in between that is not covered by any other vertex star of f . So if we impose the same conditions on the other faces as well, this region cannot be covered by Gauss images of other vertex stars unless they overlap with the Gauss image around the face f . So the Gauss images of vertex stars around a face generically do not intersect.

Proposition 8. *Assume that $K(\mathbf{v}) > 0$ and that the Gauss image $g(\mathbf{v})$ has no self-intersections for any vertex \mathbf{v} of the interior face f . If the interior angles of $g(\mathbf{v})$ at \mathbf{n}_f add up to 2π , there are exactly the following options for the shape of f and the location of the vertices where f is an inflection face:*

- (i) f is a pseudo-quadrilateral and f is an inflection face exactly in the vertex stars of its corners;
- (ii) f is a pseudo-triangle and f is an inflection face exactly in the vertex stars of its three corners and in one further vertex;
- (iii) f is a pseudo-triangle and f is an inflection face exactly in the vertex stars of two of its corners.

Proof. $\alpha_{\mathbf{v}}$ denotes the interior angle of f at one of its n vertices \mathbf{v} . By Lemma 1, the interior angle of the Gauss image of the star of $\mathbf{v} \sim f$ at \mathbf{n}_f equals

$$2\pi - (\pi - \alpha_{\mathbf{v}}) = \alpha_{\mathbf{v}} + \pi \text{ if } \alpha_{\mathbf{v}} < \pi \text{ and } f \text{ is not an inflection face at } \mathbf{v},$$

$$2\pi - (2\pi - \alpha_{\mathbf{v}}) = \alpha_{\mathbf{v}} \text{ if } \alpha_{\mathbf{v}} < \pi \text{ and } f \text{ is an inflection face at } \mathbf{v},$$

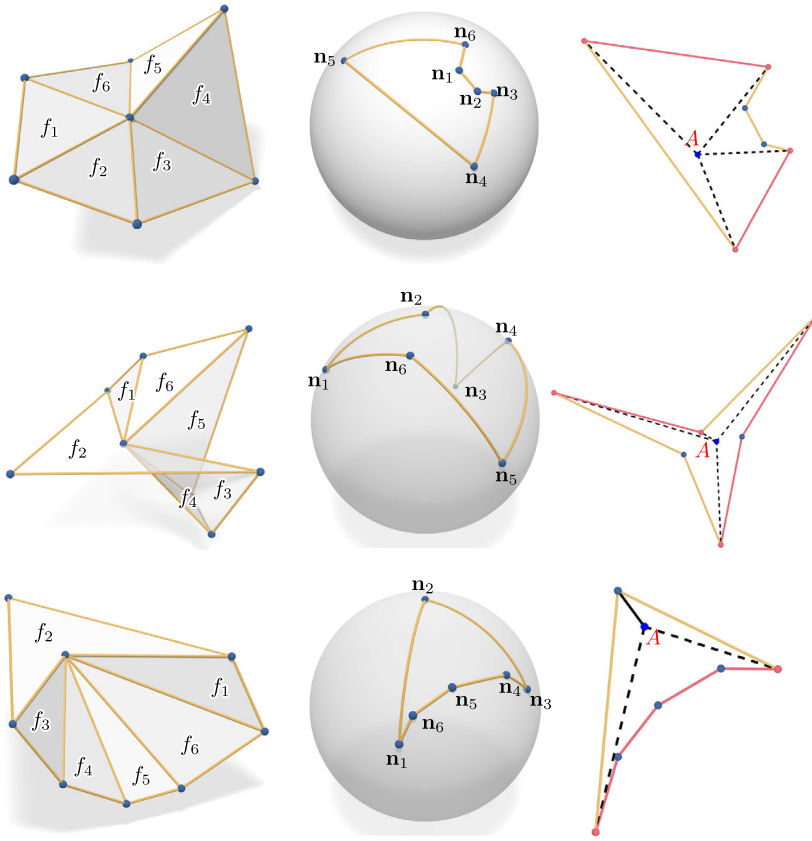


Fig. 17. Three cases for planar faces in negatively curved regions and their projective duals in Theorem 2. Vertices where the face is an inflection face are colored red and separate different colored edges. The two colors of edges correspond to adjacent faces that lie below or above the face. Asymptotic directions are marked by dashed lines. In the lower-right picture, the solid line corresponds to two asymptotic directions. (To view the colors in the figures, the reader is referred to the web version of this article.)

$$2\pi - (3\pi - \alpha_{\mathbf{v}}) = \alpha_{\mathbf{v}} - \pi \text{ if } \alpha_{\mathbf{v}} > \pi \text{ and } f \text{ is not an inflection face at } \mathbf{v},$$

$$2\pi - (2\pi - \alpha_{\mathbf{v}}) = \alpha_{\mathbf{v}} \text{ if } \alpha_{\mathbf{v}} > \pi \text{ and } f \text{ is an inflection face at } \mathbf{v}.$$

Let $c_i, i = 1, 2, 3, 4$, be the number of vertices that correspond to the i th line in the list above. Then,

$$2\pi = \sum_{\mathbf{v} \sim f_1} \alpha_{\mathbf{v}} + c_1\pi - c_3\pi = (n - 2)\pi + c_1\pi - c_3\pi.$$

It follows that $c_1 - c_3 = 4 - n$. Now, $c_1 + c_2 + c_3 + c_4 = n$, such that

$$2c_1 + c_2 + c_4 = 4.$$

Since f is planar, it has to have at least three corners, i.e., $c_1 + c_2 \geq 3$. We end up with the three cases of the proposition that are illustrated in Fig. 17:

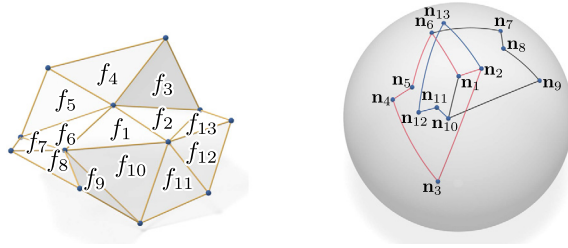


Fig. 18. Polyhedral monkey saddle at f_1 : f_1 and f_8 are not inflection faces in the left vertex star, f_1 and f_{11} are not inflection faces in the right vertex star, and f_1 and f_5 are not inflection faces in the upper vertex star.

- (i) $c_1 = 0, c_2 = 4, c_3 = n - 4, c_4 = 0$: f is a pseudo-quadrilateral and f is an inflection face exactly in the vertex stars of its corners;
- (ii) $c_1 = 0, c_2 = 3, c_3 = n - 4, c_4 = 1$: f is a pseudo-triangle and f is an inflection face exactly in the vertex stars of its three corners and in one further vertex;
- (iii) $c_1 = 1, c_2 = 2, c_3 = n - 3, c_4 = 0$: f is a pseudo-triangle and f is an inflection face exactly in the vertex stars of two of its corners. \square

Remark. If we allow the interior angles of Gauss images $g(\mathbf{v})$ to add up at \mathbf{n}_f to multiples of 2π , we can model polyhedral versions of a monkey saddle and higher order saddles. In the case of a smooth monkey saddle, a parabolic point p is surrounded by points of negative curvature. The Gauss image of a neighborhood of p has a branching of order two at the normal of p . Such a behavior can be observed in Fig. 18 as well: All faces adjacent to $f = f_1$ lie on the same side of the plane through f and all vertices incident to f have a negative discrete Gaussian curvature. In the Gauss image, we see a branching of order two at $\mathbf{n}_f = \mathbf{n}_1$. Compared to the polyhedral monkey saddle Banchoff described in [1], the parabolic point in our setup is located on the face and not on a vertex. For a polygon f with more than just three vertices and branchings in the Gauss image of higher order, corresponding higher order saddles can be modeled as well.

Since isolated parabolic points are not generic, we do not include them in our notion of smoothness. The corresponding deformation of the polyhedral monkey saddle is the replacement of f_1 by a pyramid over f_1 . Then, we get a convex vertex star at the top of the pyramid and three ordinary saddles at the three original vertices of f_1 .

In the case that the face f is even star-shaped, we are able to define discrete asymptotic directions in the point of contact of the plane through f :

Definition. Let the interior face f satisfy the conditions of Proposition 8 and be star-shaped with respect to an interior point A . A is said to be a *point of contact* of the *discrete tangent plane* given by the plane through f . *Discrete asymptotic directions* are given by the line segments connecting A with the vertices of f where f is an inflection face. In the case that there are just two such vertices, the line segment connecting A with the other corner of f counts as two discrete asymptotic directions.

Note that our discrete asymptotic directions, either defined at vertices or in faces, do not form pairs of two lines in general. Hence, it is more adequate to consider these asymptotic directions as discrete asymptotic curves passing through a vertex or a point A in a face. In the following, we justify our definition of discrete asymptotic directions in the point of contact A . The reason to choose A in such a way that f is star-shaped with respect to A is that this allows to connect A to the vertices of f with line segments inside f .

According to our discussion in Section 2.3, the discrete asymptotic direction that connects A with a vertex $\mathbf{v} \sim f$ where f is an inflection face is a possible discrete asymptotic direction in \mathbf{v} . In contrast, the line segment that counts as two discrete asymptotic direction is not a discrete asymptotic direction at the vertex. However, we will see later in Theorem 13 that the discrete asymptotic directions in this degenerate case are the projective duals of the discrete asymptotic directions in the shape discussed in case (iii) of Theorem 2 with two inflection faces, see Fig. 12.

Let us consider the intersections of planes parallel and either slightly above or below f with a neighborhood of f and their limit if the plane converges to f . If f is a pseudo-quadrilateral, then we obtain a discrete hyperbola consisting of two opposite pseudo-edges of f in the limit, see the upper-right picture in Fig. 17. The discrete asymptotic directions are kind of their asymptotes. The case of f being a pseudo-triangle with two vertices where f is an inflection face can be seen as a degenerate case where one pseudo-edge of the pseudo-quadrilateral collapses to a vertex, see the lower-right picture in Fig. 17. Finally, in the case that f is a pseudo-triangle with four vertices where it is an inflection face, then the middle-right picture in Fig. 17 shows that we still get discrete hyperbolas in the limit, though one branch of one hyperbola and one of the other form together a branch of a discrete hyperbola. At least the three discrete asymptotic directions connecting A with vertices with a convex angle discretize the asymptotes.

Remark. In the case of a simplicial surface of negative curvature, we are always in the degenerate case that is depicted in the lower-right picture in Fig. 17. This also explains why we observed in experiments that the construction of smooth simplicial surfaces is quite difficult.

3.3. Region of mixed discrete Gaussian curvature

We come to the case that the sign of $K(\mathbf{v}) \neq 0$ is not the same for all vertices $\mathbf{v} \sim f$, but the Gauss images $g(\mathbf{v})$ still have no self-intersections. If we go along the boundary of f in counterclockwise direction, the Gauss images $g(\mathbf{v})$ arrange in counterclockwise order if $K(\mathbf{v}) > 0$ and in clockwise order otherwise. In a smooth discretization, the number of overlaps should be as small as possible, so we demand that the sign of curvature changes at only two edges e_1, e_2 . This separates the boundary of f into two polylines of vertices with only positive or negative discrete Gaussian curvature, respectively.

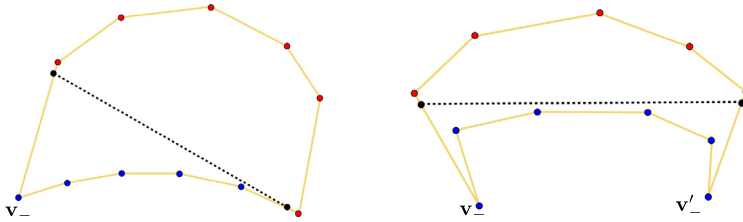


Fig. 19. “Building blocks” of faces of mixed discrete Gaussian curvature and discrete parabolic curve (dashed). Vertices of positive discrete Gaussian curvature are colored red, the others blue. The face on the left has no vertices where it is an inflection face, the face on the right is an inflection face exactly at \mathbf{v}_- and \mathbf{v}'_- .

In order to define a discrete parabolic curve as a line segment inside f , we ask in addition for the existence of a line segment connecting e_1 and e_2 that lies inside f . This implies that the polyline of all edges with a positively curved vertex has a total turning angle of less than 2π . Since the total turning angle equals the sum of interior angles $\pi - \alpha_{\mathbf{v}}$ of the respective Gauss images at \mathbf{n}_f , this means that the Gauss images of positively curved vertex stars do not cover the whole neighborhood of f . This property is favorable since it minimizes the number of overlaps. It is natural to assume the same for the Gauss images of negatively curved vertex stars, or equivalently, balancedness of the contributions of positive and negative discrete Gaussian curvature: The sum of oriented interior angles of Gauss images at \mathbf{n}_f should be zero. Note that the corresponding behavior of balancedness is observed along a parabolic curve on a generic smooth surface.

Proposition 9. *Assume that the sign of $K(\mathbf{v}) \neq 0$ changes at exactly two edges e_1, e_2 of f and that the Gauss image $g(\mathbf{v})$ has no self-intersections for any vertex \mathbf{v} of the interior face f . In addition, we assume that there exists a line segment connecting e_1 and e_2 that lies inside f and that the interior angles of the Gauss images of the corresponding vertex stars add up to 0 at \mathbf{n}_f if they are oriented according to the sign of discrete Gaussian curvature.*

Then, by adding additional vertices of zero discrete Gaussian curvature if necessary, f can be split into parts that are pseudo-polygons with at most one non-trivial pseudo-edge, see Fig. 19. Each of the new parts is an inflection face either at no vertex or at the two corners of the pseudo-edge. In the first case, one of the corners is of negative discrete Gaussian curvature, in the second case both corners are. These corners are exactly the vertices of f where the discrete Gaussian curvature is negative and the interior angle is convex. All other vertices with a convex interior angle are of positive discrete Gaussian curvature.

Proof. Let $\alpha_{\mathbf{v}}$ denote the interior angle of f at \mathbf{v} . By Lemma 1, the corresponding oriented interior angle of $g(\mathbf{v})$ at \mathbf{n}_f equals $\pi - \alpha_{\mathbf{v}}$ if $K(\mathbf{v}) > 0$. If $K(\mathbf{v}) < 0$, then we get the negatives of the angles listed in Section 3.2. Let us use the notation of c_i that we have established there, and let us denote by n_+, n_- the number of vertices of f with positive and negative discrete Gaussian curvature, respectively. Our condition for balancedness then translates to

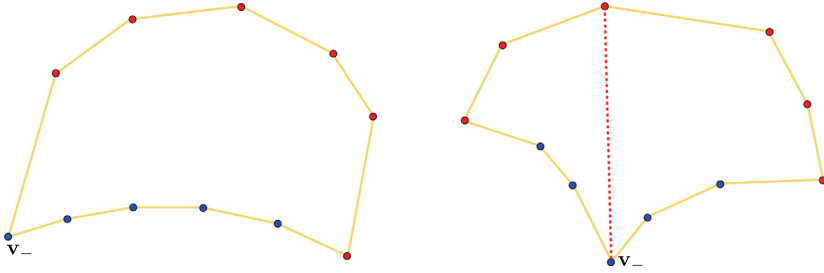


Fig. 20. Two possible shapes of f in the case $c_1 = 1$. The right shape can be split along the dotted line into two faces of the left shape.

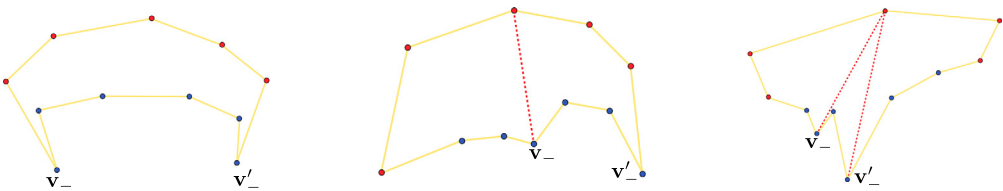


Fig. 21. Three possible shapes of f in the case $c_1 = c_4 = 0$. The middle and the right shape can be split along the dotted lines into faces that are of the shapes depicted in Fig. 19.

$$0 = n_+ \pi - \sum_{\mathbf{v} \sim f_1} \alpha_{\mathbf{v}} - c_1 \pi + c_3 \pi = (n_+ - n_+ - n_- + 2 - c_1 + c_3) \pi$$

$$\Rightarrow n_- - 2 = c_3 - c_1.$$

Moreover, $c_1 + c_2 + c_3 + c_4 = n_-$. Thus, $2c_1 + c_2 + c_4 = 2$ and c_1 can be only zero or one.

Let us start with the case $c_1 = 1$. Then, $c_2 = c_4 = 0$ and $c_3 = n_- - 1$. It follows that f_1 is never an inflection face at one of its vertices and that there is only one vertex \mathbf{v}_- with $K(\mathbf{v}_-) < 0$ that has a convex angle. Since the polyline of all edges with a positively curved vertex has a total turning angle of less than 2π , we see that f is a pseudo- $(n_+ + 1)$ -gon. If \mathbf{v}_- is adjacent to a vertex of positive curvature, then we obtain the left shape in Fig. 19. Otherwise, f has two non-trivial pseudo-edges and can be divided along \mathbf{v}_- into two such faces, see Fig. 20. For this, it may be necessary to add an additional vertex of zero discrete Gaussian curvature.

We now come to the case $c_1 = 0$. Then, $c_2 + c_4 = 2$ and $c_3 = n_- - 2$. Since the interior angles of $g(\mathbf{v})$ with $K(\mathbf{v}) < 0$ add up to less than 2π , $c_4 \leq 1$.

We start with the case $c_4 = 0$ and $c_2 = 2$. Then, f_1 is an inflection face at two of its vertices $\mathbf{v}_-, \mathbf{v}'_-$ whose interior angles are less than π . All other vertices of negative discrete Gaussian curvature have a reflex angle. Thus, f is a pseudo- $(n_+ + 2)$ -gon with three options for the positions of $\mathbf{v}_-, \mathbf{v}'_-$: Both, one, or none of them are adjacent to vertices of positive discrete Gaussian curvature, see Fig. 21. In the first case, we already have the right shape in Fig. 19; in the second case, we can split f along the vertex \mathbf{v}_- that is not adjacent to a vertex of positive curvature into one face of the left and one of

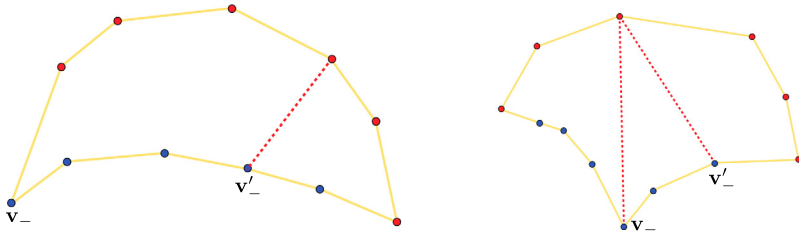


Fig. 22. Two possible shapes of f in the case $c_1 = 0, c_4 = 1$. f is an inflection face at v_- and v'_- . f can be split along the dotted lines into the parts of Fig. 19.

the right shape in Fig. 19; in the last case, we can split f along v_-, v'_- into two faces of the left and one of the right shape in Fig. 19. Note that only one of the two parts at v_- or v'_- inherits the inflection-property in such a way that the number of inflections around each part is still even.

We are left with the case $c_2 = c_4 = 1$. Then, f_1 is an inflection face at two of its vertices. At one vertex v_- , the interior angle is less than π , at the other v'_- , it is greater than π . Thus, we obtain the shapes of Fig. 20. But now, f_1 is an inflection face at v_- and v'_- , see Fig. 22. We can divide the faces along the dotted lines into two or three parts corresponding to those in Fig. 19. The reflex angle at v'_- splits into two convex angles. We assign the inflection-property of each of the vertices to just one of the two incident parts in such a way that we indeed obtain the situation of Fig. 19. \square

Definition. Let f be an interior face of P that has exactly two edges whose incident vertices have a different sign of discrete Gaussian curvature. If these edges can be connected by a line segment that is contained in f , it is called a *discrete parabolic curve*.

Let us shortly discuss the relation between parabolic curves and asymptotic directions. If the points of a parabolic curve on a smooth surface have a common tangent plane (e.g. on a torus), then the parabolic curve envelopes the asymptotic lines [3]. We know from our discussion in Section 2.3 that the discrete asymptotic directions in all vertices of f of negative discrete Gaussian curvature that are not corners of f and where f is not an inflection face lie in the double cone spanned by an incident edge and the inverse of the other. Furthermore, discrete asymptotic directions in the corners of f , supposing that f is an inflection face there, lie in the cone spanned by the incident edges. Hence, the discrete parabolic curve envelopes the discrete asymptotic directions in the two building blocks depicted in Fig. 19.

If the parabolic curve on a smooth surface has a variable tangent plane, then the asymptotic lines have cusps along the parabolic curve [3]. Looking at the right picture in Fig. 20, the discrete asymptotic directions along the two pseudo-edges come together at v_- , so we actually have a cusp-like behavior. Being in analogy to the smooth case, the tangent plane should change there, which is modeled by the division of f into two parts along the dotted line. The partitions shown in Figs. 21 and 22 can be motivated in a similar way.

3.4. Smooth polyhedral surfaces

We are now ready to give our definition of a smooth polyhedral surface.

Definition. Let P be an orientable polyhedral surface immersed into three-dimensional Euclidean space. Let V and F denote the sets of interior vertices and faces of P , respectively.

- Let $K(\mathbf{v}) > 0$ for all $\mathbf{v} \in V$. Then, P is a (*positively curved*) *smooth polyhedral surface* if for each $\mathbf{v} \in V$, the Gauss image $g(\mathbf{v})$ has no self-intersection.
- Let $K(\mathbf{v}) < 0$ for all $\mathbf{v} \in V$. Then, P is a (*negatively curved*) *smooth polyhedral surface* if for each $\mathbf{v} \in V$ and $f \in F$:
 - (i) f is star-shaped;
 - (ii) the Gauss image $g(\mathbf{v})$ is star-shaped with respect to an interior point and contained in an open hemisphere;
 - (iii) the interior angles of $g(\mathbf{v}')$, $\mathbf{v}' \sim f$, at the normal \mathbf{n}_f sum up to 2π .
- P is a *smooth polyhedral surface* if for each $\mathbf{v} \in V$ and $f \in F$:
 - (i) $K(\mathbf{v}) \neq 0$;
 - (ii) the Gauss image $g(\mathbf{v})$ is star-shaped with respect to an interior point and contained in an open hemisphere;
 - (iii) when $K(\mathbf{v}')$ has the same sign for all vertices $\mathbf{v}' \sim f$, f is star-shaped and the interior angles of $g(\mathbf{v}')$ at the normal \mathbf{n}_f sum up to 2π ;
 - (iv) when $K(\mathbf{v}')$ has not the same sign for all vertices $\mathbf{v}' \sim f$, f has exactly two edges $\mathbf{v}_1\mathbf{v}'_1$ and $\mathbf{v}_2\mathbf{v}'_2$ with $K(\mathbf{v}_i) > 0 > K(\mathbf{v}'_i)$, the interior angles of $g(\mathbf{v}')$ at the normal \mathbf{n}_f sum up to 0 if they are oriented according to the sign of $K(\mathbf{v}')$, and the line segment $\mathbf{v}_1\mathbf{v}_2$ is contained in f .

Remark. We remark that our definition of a positively curved smooth polyhedral surface is not different from the definition of a smooth polyhedral surface with $K(\mathbf{v}) > 0$ for all $\mathbf{v} \in V$. Indeed, if all Gauss images $g(\mathbf{v})$ of a positively curved surface have no self-intersections, then they are star-shaped, contained in an open hemisphere, and their interior angles at a normal vector sum up to 2π by Propositions 5 and 7.

Our intuition behind a smooth polyhedral surface that is either positively or negatively curved is a surface whose Gauss image defines locally a nice cellular decomposition of the sphere. The cells $g(\mathbf{v})$ shall be not too large, meaning that they are contained in open hemispheres. At each vertex of the Gauss image, which is the normal of a face, the cells shall arrange without an overlap near the vertex. Finally, the cells shall be star-shaped, such that they have no self-intersections. Star-shapedness allows to define discrete asymptotic directions at vertices \mathbf{v} with $K(\mathbf{v}) < 0$. For a similar reason, we demand star-shapedness of faces in the case of negative curvature.

When the sign of discrete Gaussian curvature changes at a face f , we want to define a line segment as the discrete parabolic curve. That is why we assume exactly two sign

changes to happen along the edges of f , and it should be possible to connect these two edges with a line segment inside the face. Furthermore, the contributions of positive and negative discrete Gaussian curvature around f shall be balanced, so we ask the interior angles of the Gauss images at \mathbf{n}_f to sum up to zero if they are oriented according to the sign of curvature.

Theorem 2 (i) to (iii) describes the possible shapes of Gauss images of vertex stars of smooth polyhedral surfaces P ; Propositions 7, 8, and 9 describe the shapes of faces of P in the cases of positive, negative, and mixed discrete Gaussian curvature, respectively.

Discrete tangent planes at vertices are given by the planes orthogonal to vectors with respect to which the Gauss image of the vertex star is star-shaped, discrete normals by the poles of open hemispheres containing the Gauss image, and the points of contact of the face tangent planes are points with respect to which the face is star-shaped (assuming that the sign of discrete Gaussian curvature does not change). Discrete asymptotic directions were discussed in Sections 2.3 and 3.2, a discrete parabolic curve was defined in Section 3.3.

3.5. Comparison between a smooth surface and its discretizations

Our discussion of the shapes of faces of a smooth polyhedral surface explains the transformations of shapes that occurred in the examples generated in [5]. Let us have a closer look at a Dupin cyclide and two smooth discretizations of it. One of the polyhedral surfaces in Fig. 23 consists of triangles only, the other realizes the dual situation of having only vertices of valence three.

In the case of the polyhedral surface consisting of hexagons, we can see how the shapes of the faces adapt to the sign of curvature exactly as we described in the previous sections. The hexagons are convex if the curvature is positive, they are pseudo-quadrilaterals if the curvature is negative, and along the discrete parabolic curve we recognize the shapes of Fig. 19.

For both discrete cyclides, the discrete parabolic curves are close to the smooth parabolic curve. Having the freedom in locating the vertices of the discrete parabolic curve in mind, we could have aligned discrete and smooth parabolic curves even better.

When we come to the comparison of asymptotic directions, we see that the discrete asymptotic directions align very well with the asymptotic curves in the case of the triangulated surface. For the polyhedral surface with vertices of valence three, we are always in the situation of Fig. 12. That means that two asymptotic directions are collinear. If we ignore them and consider for each vertex the other two discrete asymptotic directions only, we obtain a good accordance with the asymptotic directions of the smooth cyclide. Dual to this case is the situation described in the lower-right picture of Fig. 17 and that is exactly what we observe on the triangulated surface. If we had depicted the discrete asymptotic directions inside faces, the line segments connecting a central point of contact with the vertices where the triangle is an inflection face would align with the smooth

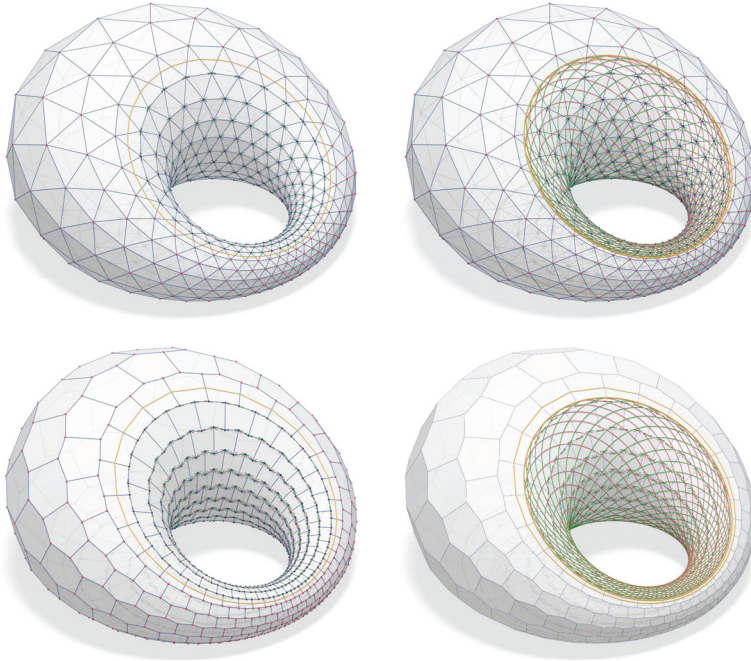


Fig. 23. Two smooth polyhedral surfaces that discretize a Dupin cyclide. The yellow polylines are discrete parabolic curves; at each vertex, four discrete asymptotic directions are drawn in red and green. The right hand side shows overlaps of the discrete and the smooth images. We can see the alignment of the discrete parabolic curve and the discrete asymptotic directions with the smooth parabolic curve (yellow) and the corresponding two families of asymptotic curves (red and green).

asymptotic curves, but the line segment counting as two discrete asymptotic directions would not. Again, it is reasonable to ignore these two directions.

4. Projective transformations

We study projective transformations of polyhedral surfaces and how they affect smoothness. When we compare our discussions for smoothness around a vertex and around a face, we observe several analogies: On the one hand, the Gauss image of a positively or negatively curved smooth vertex star is either a convex spherical polygon or a spherical pseudo- n -gon ($n = 3, 4$), respectively. On the other hand, a face of a positively or negatively curved smooth polyhedral surface is either a convex polygon or a pseudo- n -gon ($n = 3, 4$), respectively. Such properties hint at an invariance of our notion with respect to correlations in projective geometry. In particular, our notion of smoothness should be already invariant under projective transformations that do not map any point of the surface to infinity.

Theorem 10. *Let P be a smooth polyhedral surface immersed into Euclidean space that we consider as the space of finite points in three-dimensional projective space. Let π be a projective transformation (collineation) that does not map any point of P to infinity.*

Then, $\pi(P)$ is a smooth polyhedral surface. Discrete normals, discrete tangent planes, discrete asymptotic directions, discrete parabolic curves, and points of contact are mapped to the corresponding objects of $\pi(P)$.

Proof. Since the faces incident to a vertex \mathbf{v} of P did not intersect in a neighborhood of \mathbf{v} , their images will not intersect in a neighborhood of $\pi(\mathbf{v})$. In particular, $\pi(P)$ is immersed in three-dimensional Euclidean space.

Let us investigate how the Gauss image of the star of \mathbf{v} changes. The normal vectors of incident faces are defined by the edges emanating from \mathbf{v} . So the change of the Gauss image is encoded in the change of an infinitesimal neighborhood of the vertex. If we differentiate π at a vertex \mathbf{v} of P , we obtain an affine transformation ρ . For this, note that π does not map points of P to infinity.

ρ is a concatenation of a bijective linear transformation and a translation. The translation does not affect the Gauss image, so we assume that ρ is a linear transformation of non-vanishing determinant. Since the negative of the identity matrix defines just a point reflection in the origin, we may assume that ρ is orientation-preserving. Noting that the general linear group has exactly two connected components that are distinguished by the sign of determinant, there is a continuous curve γ in this space connecting the identity with ρ . Each point of γ then defines an affine transformation.

If we move along γ , the image of the polyhedral surface and its Gauss images change continuously. In particular, if $g(\pi(\mathbf{v}))$ has a self-intersection but $g(\mathbf{v})$ has not, then somewhere on γ there is an affine transformation that generates a Gauss image where three normals lie on a common great circle. The planes passing through the arcs in the Gauss image and the origin are orthogonal to the corresponding edge in the star of the vertex. If three normals lie on a common great circle, then two faces become coplanar or two edges possess a common orthogonal plane, i.e., they become collinear. Both cannot happen under a linear transformation of non-vanishing determinant. It follows that $g(\pi(\mathbf{v}))$ is free of self-intersections. Furthermore, the sign of discrete Gaussian curvature does not change.

Since P possesses a transverse plane at \mathbf{v} , there exists $\mathbf{n}' \in S^2$ such that a disk neighborhood of \mathbf{v} projects to a plane orthogonal to \mathbf{n}' in a one-to-one way. We want to prove that $\rho(\mathbf{n}')/|\rho(\mathbf{n}')|$ does the same for $\pi(\mathbf{v})$.

If a disk neighborhood of \mathbf{v} projects to a plane orthogonal to \mathbf{n}' in a one-to-one way, then it bijectively projects to any plane that is not parallel to \mathbf{n}' , as long as the direction of projection is parallel to \mathbf{n}' . Equivalently, any line parallel to \mathbf{n}' and close to \mathbf{v} intersects the disk neighborhood in exactly one point. The linear transformation ρ preserves parallelity and incidences. It follows that a disk neighborhood of $\pi(\mathbf{v})$ bijectively projects to any plane that is not parallel to $\rho(\mathbf{n}')$. Due to the continuity argument above, $\rho(\mathbf{n}')/|\rho(\mathbf{n}')|$ lies inside $g(\pi(\mathbf{v}))$. In particular, $\rho(\mathbf{n}')/|\rho(\mathbf{n}')|$ is a discrete normal.

If the discrete Gaussian curvature is positive, then the Gauss image $g(\pi(\mathbf{v}))$ is star-shaped by Proposition 5. In the case of negative discrete Gaussian curvature, we apply

Theorem 6: Star-shapedness of the Gauss image is equivalently described by the property that a band of parallel planes intersect the vertex star in discrete hyperbolas. By assumption, the planes parallel to the discrete tangent plane E_0 intersect the star of \mathbf{v} in discrete hyperbolas. We argue that this is also the case for the planes parallel to $\rho(E_0)$ and the star of $\pi(\mathbf{v})$.

Each linear transformation on the curve γ maps the planes parallel to E_0 to a band of planes parallel to the image of E_0 . When we move along γ , then their intersections with the star of the vertex change continuously. If they are not all discrete hyperbolas, then an edge in a polyline collapses or two adjacent edges become parallel at some point. In the first case, a face of the vertex star does not intersect the band of planes any longer; in the second case, two faces become coplanar. Both situations cannot occur for an affine transformation. It follows that $g(\pi(\mathbf{v}))$ is star-shaped and that discrete tangent planes are mapped to discrete tangent planes. Also, discrete asymptotic directions at vertices are mapped to discrete asymptotic directions.

We have proven that the star of $\pi(\mathbf{v})$ is smooth, so we are left with the situation around faces. We have already shown that the sign of discrete Gaussian curvature does not change. In particular, the number of edges of a face where the sign changes remains invariant. Clearly, star-shaped faces remain star-shaped: f is star-shaped with respect to A if and only if all line segments connecting A with one of the vertices of f lie completely in f . Since π does not map any point of f to infinity, $\pi(f)$ will be star-shaped with respect to $\pi(A)$. It follows that points of contact and discrete asymptotic directions inside faces are mapped to their counterparts in the projective image.

The main criterion for smoothness around faces f is that the interior angles of the Gauss images at \mathbf{n}_f sum up to 2π if all incident vertices have the same sign of discrete Gaussian curvature. If the signs of discrete Gaussian curvature differ, then we demand that the sum of suitably oriented interior angles of Gauss images is zero. Proposition 7 implies the case of positive curvature. For the cases of negative and mixed discrete Gaussian curvature, the computation of these sums in Sections 3.2 and 3.3 relied on Lemma 1, which only made use of the properties of the face f having an angle greater or less than π and being an inflection face or not at $\mathbf{v} \sim f$. It follows that the sum of interior angles does not change if we show that these two properties remain invariant under the projective transformation π .

An angle α_f of a face f is less than π if and only if there exists a line segment connecting the two edges inside f . The image of that line segment under π will be again a line segment connecting the two image edges. Since π does not map any point of P to infinity, that line segment will be contained in $\pi(f)$.

A face f is an inflection face for a vertex $\mathbf{v} \sim f$ if and only if there exist lines l arbitrarily close to \mathbf{v} that intersect f and both its neighboring faces. The lines $\pi(l)$ will then intersect $\pi(f)$ and both its neighboring faces and are arbitrarily close to $\pi(\mathbf{v})$.

To complete the proof that $\pi(P)$ is a smooth polyhedral surface provided that P is, we have to show that if the image face $\pi(f)$ contains vertices of both positive and negative discrete Gaussian curvature, then the line segment connecting the two positively curved

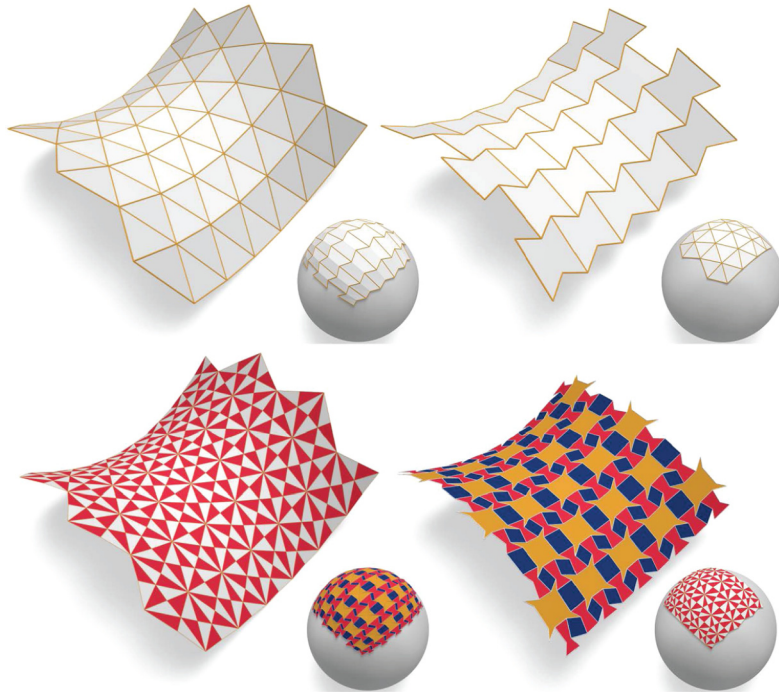


Fig. 24. Dual pairs of negatively curved polyhedral surfaces and their Gauss images.

vertices that are adjacent to negatively curved vertices is contained in $\pi(f)$. But this is clearly the case since the face f has this property and π does not map any point of f to infinity. By the same argument, the discrete parabolic curve is mapped to a discrete parabolic curve of the image. \square

We conclude with investigating polyhedral surfaces P^* that are projective duals of P . Numerical experiments show an interesting phenomenon, see Fig. 24: The Gauss image of a smooth polyhedral surface P of negative discrete Gaussian curvature looks like the projection of a smooth realization of the dual polyhedral surface P^* , and vice versa. This observation can be made precise:

Theorem 11. *Let P be a smooth polyhedral surface of either positive or negative discrete Gaussian curvature. If its Gauss image is contained in an open hemisphere, then it can be obtained by projecting a dual polyhedral surface P^* to S^2 . This dual surface is smooth, has the same sign of curvature as P , and the projection center agrees with the center O of the Gaussian sphere S^2 .*

Proof. For each vertex \mathbf{v} of P , we consider the set of planes that are passing through \mathbf{v} and whose normal vectors lie in $g(\mathbf{v})$. We choose the point O in such a way that a unit sphere centered at O does not intersect any of these planes. This is possible since the Gauss image is contained in a hemisphere: Let \mathbf{n} be the pole of such a hemisphere and

consider a ray r with direction $-\mathbf{n}$ that starts in an interior point of a face of P . Due to our assumption, none of the above planes can be parallel to r . Hence, a point O far away on r will satisfy the condition we are looking for. We put the origin of the coordinate system to O and place the center of S^2 there.

By definition, the tangent planes G_f of S^2 at Gauss image points \mathbf{n}_f are parallel to the planes P_f of the faces f of P . Let us now apply the polarity Π with respect to S^2 . The polyhedral surface P is mapped to a dual polyhedral surface P^* . The vertices \mathbf{v}_f^* of P^* are the polar images of the face planes P_f (as P_f does not pass through O , \mathbf{v}_f^* is not at infinity). Tangent planes G_f of S^2 are mapped via Π to their contact points \mathbf{n}_f . Parallel planes are mapped to points on a line through the center O of S^2 . Thus, for each face f , the points \mathbf{v}_f^* , \mathbf{n}_f , and O are collinear. By our choice of the position of O , \mathbf{v}_f^* always lies in between O and \mathbf{n}_f . Hence, the Gauss image of P is generated by projecting the polar mesh P^* from O onto S^2 .

Since the interior angles of the Gauss images of P add up to 2π at \mathbf{n}_f , the plane with normal \mathbf{n}_f passing through \mathbf{v}_f^* serves as a transverse plane for the star of \mathbf{v}_f^* . The faces of P^* are star-shaped because the Gauss images of vertex stars of P are star-shaped.

Let us apply the projective duality Π again to get a map from P^* to $P^{**} = P$. By our observations above, the Gauss image of P^* is obtained by projecting P from O onto S^2 , and the plane passing through a vertex \mathbf{v} that is orthogonal to the line $O\mathbf{v}$ is a transverse plane. We deduce that the interior angles of the Gauss images of P^* add up to 2π at $\mathbf{n}_{\mathbf{v}^*}$. Furthermore, the Gauss images of vertex stars of P^* are star-shaped since the faces of P are.

Since the Gauss images of the vertex stars of P^* have non-vanishing area, the discrete Gaussian curvature of P^* is nowhere vanishing. When we consider the dual surface, the orientation changes if the curvature is negative and stays the same if it is positive. The dual of the dual surface has again the original orientation, so the sign of curvature has to be the same for P and P^* . \square

Proposition 12. *Let P be a smooth polyhedral surface such that there exists a finite point that does not lie in any plane that is orthogonal to a normal vector contained in the Gauss image of P and passing through the corresponding vertex of P . Let P^* be its dual as in Theorem 11.*

Then, if f is an inflection face at the vertex $\mathbf{v} \sim f$, then the face of P^ dual to \mathbf{v} is an inflection face at the vertex \mathbf{v}_f^* dual to f (and vice versa).*

Proof. The key of the proof is Lemma 1. If the angle α_f of f at \mathbf{v} is a reflex angle, then by Theorem 2, we are in the setting of negative discrete Gaussian curvature. Due to Theorem 11, P^* is also negatively curved. Lemma 1 then shows that the angle $\alpha_{\mathbf{v}^*}$ of the face dual to \mathbf{v}^* at the vertex \mathbf{v}_f^* is greater than or less than π if f is an inflection face or not, respectively. Note that the angle $\alpha_{\mathbf{v}^*}$ generally does not coincide with the corresponding spherical angle at \mathbf{n}_f . Due to the orientation change in the case of negative curvature, this spherical angle equals $2\pi - \alpha'_f$ in Lemma 1.

If $\alpha_{\mathbf{v}}^* > \pi$, we have a reflex angle $\alpha_{\mathbf{v}}^*$ whose dual angle is also a reflex angle. By Lemma 1, the face dual to \mathbf{v} is then an inflection face at \mathbf{v}_f^* . If $\alpha_{\mathbf{v}}^* < \pi$, $\alpha_{\mathbf{v}}^*$ is convex and its dual angle is not. It follows from Lemma 1 that the face dual to \mathbf{v} is not an inflection face at \mathbf{v}_f^* .

Let us now assume that $\alpha_f < \pi$. If f is an inflection face, then we are again in the setting of negative curvature. Using that the dual angle is also convex, we conclude that the face dual to \mathbf{v} is an inflection face at \mathbf{v}_f^* .

If f is not an inflection face and the discrete Gaussian curvature is negative or positive, then the dual angle is a reflex or a convex angle, respectively. Since the dual of the dual angle is convex, we use again Lemma 1 to deduce that the face dual to \mathbf{v} is not an inflection face at \mathbf{v}_f^* . \square

We can combine Theorem 11 with Theorem 10 to show that the projective dual surface of an either positively or negatively curved smooth polyhedral surface is smooth for more general correlations than the one we used in Theorem 11:

Theorem 13. *Let P be a smooth polyhedral surface of either positive or negative discrete Gaussian curvature. We assume that there exists a finite point that does not lie in any plane that passes through a vertex \mathbf{v} of P and has a normal contained in $g(\mathbf{v})$. Let Γ be a projective correlation that maps no such plane to a point at infinity.*

Then, the dual surface $P^ = \Gamma(P)$ is a smooth polyhedral surface that has the same sign of curvature as P . If E is a discrete tangent plane in \mathbf{v} , then $\Gamma(E)$ is a point of contact of the dual face \mathbf{v}^* . Conversely, $\Gamma(A)$ is a discrete tangent plane in the vertex \mathbf{v}_f^* dual to the face f of P if A is a point of contact in f . Γ maps discrete asymptotic directions to discrete asymptotic directions.*

Proof. The assumption that Γ does not map any plane tangent to P to infinity guarantees that the dual surface P^* is indeed a polyhedral surface that does not contain any point at infinity. Let Π be the polarity that we constructed in Theorem 11 and let P_{Π}^* be the corresponding dual surface. Π and Γ then define a projective transformation π that maps P_{Π}^* to P^* .

By Theorem 11, P_{Π}^* is a smooth polyhedral surface with the same sign of discrete Gaussian curvature as P , and so is P^* by Theorem 10. In addition, discrete tangent planes, points of contact, and discrete asymptotic directions are mapped to their counterparts. In particular, it is sufficient to show the duality statements for the surfaces P and P_{Π}^* . In what follows, let $P^* = P_{\Pi}^*$.

If E is a discrete tangent plane in the vertex \mathbf{v} of P , then the Gauss image $g(\mathbf{v})$ is star-shaped with respect to the normal \mathbf{n} of E that lies inside $g(\mathbf{v})$. It follows from our considerations in the proof of Theorem 10 that the dual face \mathbf{v}^* is star-shaped with respect to its intersection with the line passing through \mathbf{n} and the center of projection. So $\Pi(E)$ is indeed a point of contact.

Conversely, if A is a point of contact in the face f of P , f is star-shaped with respect to A . If we apply the polarity Π , then the Gauss image of the star of the dual vertex \mathbf{v}_f^* is star-shaped with respect to the normal of $\Pi(A)$ that lies inside the Gauss image. In particular, $\Pi(A)$ is a discrete tangent plane.

It remains to consider the discrete asymptotic directions, so we are in the case that both P and P_{Π}^* are negatively curved. Let \mathbf{v} be an interior vertex of P . Then, we defined the discrete asymptotic directions in the end of Section 2.3 as the four directions given by the four line segments in the intersection of the discrete tangent plane with a disk neighborhood of \mathbf{v} .

In the case that the vertex star contains four inflection faces, these four line segments are exactly the intersection of the discrete tangent plane with these four inflection faces. Under the polarity Π , these rays are mapped to the four rays in \mathbf{v}^* each connecting the point of contact with one of the four vertices of \mathbf{v}^* that are dual to the four inflection faces in the star of \mathbf{v} . By Proposition 12, \mathbf{v}^* is an inflection face at these four vertices. It then follows from our discussion in the end of Section 3.2 that the projective duals of the discrete asymptotic directions are again discrete asymptotic directions.

In the case that the vertex star contains only two inflection faces, two discrete asymptotic directions are the intersection of the discrete tangent plane with the two inflection faces. The other two asymptotic directions are collinear and given by the intersection with the face f that has a reflex angle. Similar to the previous paragraph, the first two discrete asymptotic directions correspond to the rays connecting the point of contact with the two corners of \mathbf{v}^* where the face is an inflection face. The latter two discrete asymptotic directions are both mapped to a ray connecting the vertex \mathbf{v}_f^* dual to f with the point of contact. Since f is not an inflection face, the interior angle of the Gauss image of the star of \mathbf{v} at \mathbf{n}_f is less than π by Theorem 2 (iii). Thus, \mathbf{v}_f^* is a corner of \mathbf{v}^* . Since we defined the line segment connecting the point of contact with that corner as two discrete asymptotic directions, we have shown that the discrete asymptotic directions in \mathbf{v} correspond to the discrete asymptotic directions in \mathbf{v}^* .

By duality, it also follows that the discrete asymptotic directions in a general face f of P correspond to the discrete asymptotic directions in the dual vertex \mathbf{v}_f^* . \square

5. Future research

In our paper we did not address questions of convergence and approximation:

- Given a sequence of smooth polyhedral surfaces converging to a smooth surface, do the discrete normal vectors, discrete tangent planes, discrete asymptotic directions, and the discrete parabolic curves converge to their smooth counterparts?
- Given a smooth surface S and $\varepsilon > 0$, is it possible to find a smooth polyhedral surface P within a ε -neighborhood of S ? Can P be chosen to be a simplicial surface? As $\varepsilon \rightarrow 0$, do some shapes of vertex stars and faces shown in Fig. 17 not occur anymore?

- In the previous papers [4,5,8], mainly the regularization of a given mesh was investigated. What is missing is an algorithm that finds a good initial mesh to start with. As was shown in these papers, the combinatorics of the polyhedral surface and the initial realization of it may prevent a successful optimization. We expect that a careful comparison of smooth and discrete asymptotic directions will be essential for finding smooth polyhedral approximations of negatively curved surfaces.

Acknowledgments

The authors are grateful to Thomas Banchoff for fruitful discussions concerning the Gauss image of a vertex star and to Günter Rote for pointing out the connection to [7]. This research was initiated during the first author's stay at the Erwin Schrödinger International Institute for Mathematical Physics in Vienna and continued during his stays at the Institut des Hautes Études Scientifiques in Bures-sur-Yvette and the Max Planck Institute for Mathematics in Bonn. The first author thanks the institutes for their hospitality and the European Post-Doctoral Institute for Mathematical Sciences for the opportunity to visit the afore mentioned research institutes. The first and last author are grateful for support by the DFG Collaborative Research Center TRR 109 "Discretization in Geometry and Dynamics" and corresponding FWF grants I 706-N26 and I 2978-N35. The first author was also partially funded by the Deutsche Forschungsgemeinschaft (DFG, German Research Foundation) under Germany's Excellence Strategy – The Berlin Mathematics Research Center MATH+ (EXC-2046/1, project ID: 390685689).

References

- [1] T. Banchoff, Critical points and curvature for embedded polyhedral surfaces, *Am. Math. Mon.* 77 (1970) 475–485.
- [2] T. Banchoff, F. Günther, The Gauss map of polyhedral vertex stars, 35 pages, preprint, arXiv: 1909.09184, 2019.
- [3] D. Hilbert, S. Cohn-Vossen, *Geometry and the Imagination*, Chelsea Pub. Co., New York, 1952, translated by P. Nemenyi.
- [4] C. Jiang, F. Günther, J. Wallner, H. Pottmann, Measuring and controlling fairness of triangulations, in: S. Adriaenssens, F. Gramazio, M. Kohler, A. Menges, M. Pauly (Eds.), *Advances in Architectural Geometry 2016*, VDF Hochschulverlag, ETH Zürich, 2016, pp. 24–39.
- [5] C. Jiang, C. Tang, A. Vaxman, P. Wonka, H. Pottmann, Polyhedral patterns, *ACM Trans. Graph.* 34 (6) (2015).
- [6] Y. Liu, H. Pottmann, J. Wallner, Y.-L. Yang, W. Wang, Geometric modeling with conical meshes and developable surfaces, *ACM Trans. Graph.* 25 (3) (2006) 681–689.
- [7] D. Orden, G. Rote, F. Santos, B. Servatius, H. Servatius, W. Whiteley, Non-crossing frameworks with non-crossing reciprocals, *Discrete Comput. Geom.* 32 (4) (2004) 567–600.
- [8] D. Pellis, M. Kilian, F. Dellinger, J. Wallner, H. Pottmann, Visual smoothness of polyhedral surfaces, *ACM Trans. Graph.* 38 (4) (2019).